Level Set Modeling of Profile Evolution during Deposition Process

Ohseob Kwon* and Taeyoung Won**
Computational Electronics Center,
School of Electrical and Computer Engineering, Inha University
253 Yonghyun-Dong, Nam-Gu, Inchon, Korea 402-751
E-mail: kos@hsel.inha.ac.kr*, twon@hsel.inha.ac.kr**

Abstract

In this paper, we report three-dimensional modeling of the sputter deposition process for ULSI interconnects. The numerical method in this work is based upon the level-set scheme for accurately tracking the moving boundaries of the deposited profiles. A new approach is proposed in an effort to reduce the calculating CPU time during the calculating step of the deposition rate. Our simulation incorporates three-dimensional direct and/or indirect flux distributions and shadow-effects as well as the dependence of sticking coefficient that affects not only the thickness of film at different position but also the initiation of the creation of a void. In this work, we present several numerical examples for copper deposition process, which include L-shaped trenches and contact holes with different aspect ratios.

1 Introduction

Sputter deposition is one of the most essential processes for forming ULSI interconnects. Due to the increasing complexity of devices and interconnects, the control of the uniformity of the deposited film thickness is required in the sub-half-micron era. Modeling and simulation of sputter deposition processes is quite important for understanding the characteristics of the topographical evolution in the reliable formation of densely packed interconnect metal lines.

In recent years, a great deal of research effort has been made on the development of three-dimensional simulator for sputter deposition process with taking the equipment modeling into account [1]. In this work, we employ the level set method [2] with the novel methods to investigate the fast and accurate modeling of the topography evolution for a deposition process.

2 Feature Profile Evolution Model

To calculate a deposition rate of each surface patches, one point 'B' in patch was selected. Fig. 1 shows that all intersection points between edge of cell and zero level set are selected. In case the zero level set is located on the edge of cell, both vertexes of edge are selected as the intersectional points. In Fig. 1, the central point

'A' was calculated using four intersectional points and then the nearest point 'B' from central point 'A' is found in zero level set. The nearest point B is used for the calculation of the deposition rate of each surface patches.

The sputter yield from the target has been calculated by Monte Carlo method with the binary encounter model [3]. The sputter yield, $Y(\Omega)=Y(\theta,\varphi)$ as a function of incident energy and incident angle, as well as the distribution of atomic emission, can be calculated for wide range of 10 eV ~ 100 keV. In this work, Ar ions, which normally incident on the copper target with energy of 1 keV, was chosen to calculate the sputter yield of copper atoms. The maximum emission of sputtered copper atoms is at 45° from the axis without azimuth dependence.

In the simulation of deposition process with low sticking coefficient, as we assumed the reflection with cosine distribution, the ratio of the flux at i-th and $(i+1)$-th reflection would converge to a constant value. Therefore, the flux at arbitrary position can be calculated when the convergence is generated at n-th reflection. The calculation of the reflected flux at arbitrary position is expressed by

$$F_{reflected}^{sum} = \sum_{i=1}^{n} F_{reflected}^{i} + \frac{F_{reflected}^{i+1}}{1 - F_{reflected}^{i+1} / F_{reflected}^{i}}$$

A novel approach to reduce the CPU time was made by reducing the number of the level set points for calculating the deposition rate. We put the deposition rate for calculating the level set equation at each grid equivalent to the deposition rate of cell including a nearest surface point from (i, j, k) grid, as shown in Fig. 2. And then, the deposition rate at all grid of narrow band is determined. Fig. 3 shows the number of points used for calculation the deposition rate to the various grid sizes. Our method has very good computational efficiency to the old method. In case width of narrow band is twice grid width, the number of points is about five times more than presented method. Therefore, for N points, it requires N^2 evaluation for calculating the deposition rate.

3 Results and Discussion

In Fig. 4 is shown the profiles for copper sputter deposition performed on L-shaped trench and contact-hole structures with the aspect ratio of '1' and '2', respectively. In this simulation, the width of trench was chosen as 0.13 μm and the size of contact-hole was chosen as 0.13 μm×0.13 μm. The flux due to the surface reflection was taken into account with an assumption that the sticking coefficient Γ is 0.5. In Fig. 4, as the aspect ratio increases, the deposited film thickness on the sidewall decreases due to the decrease of the visible solid angle. In Fig. 4(c), (d), (e) and (f), the deposited film of left side is thicker than right side. It is due to the difference of amount of incident flux, i.e., the size of the visible solid angle. In case of the results with the aspect ratio of '2', the thickness of film deposited at the

sidewall and bottom is thinner than the aspect ratio of '1'. We find that as increasing the aspect ratio, the amount of incident flux decrease.

Fig. 5(a) shows the eight different positions indicated on the cross-sectional view, AA' of L-shaped trench and on the cress-sectional view, BB' of contact hole in order to analysis the variation of the thickness ratio (i.e., ratio of the film thickness at a particular position to the flat-surface film thickness w) in Fig. 4. Fig. 5(b) and (c) illustrates the variation of the thickness ratio at eight different positions indicated in Fig. 5 as a function of normalized time and different aspect ratio of Fig. 4. The film thickness at the sidewall does not exhibit a monotonously increasing dependence on the depth of trench or the contact hole. The amount of the incoming flux is the largest at top surface, while the flux being the smallest at the corner of bottom. Therefore, the film topography on the sidewall tends to be bowed and the thickness ratio becomes worse gradually as the simulation time continues.

Fig. 6 illustrates the void creation of L-shaped trench and contact hole. The aspect ratio is '1' and '3', respectively, and, other parameters are equal to Fig. 4. In Fig. 6, the width of void at L-shape trench is smaller than at contact hole. It is because the ratio of incident flux (i.e., the bottom to the flat surface without the geometrical shadowing) at L-shape trench is bigger than at contact hole. Furthermore, the void is created earlier in a contact hole with a large aspect ratio than that with a small aspect ratio due to the visible solid angle.

4 Conclusions

In this paper, we report the topography simulator for the sputter deposition process of copper. We discussed more detail about the geometrical effects in three-dimensional simulation of the profile of a L-shape trench and a contact hole with taking into account the physical parameters such as the visible solid angle and the surface reflection. As the aspect ratio increases, the deposited film thickness on the sidewall decreases due to the decrease of visible solid angle, and it affects the time of the void creation. Additionally, the thickness ratio of overall surface becomes worse gradually as the simulation time continues.

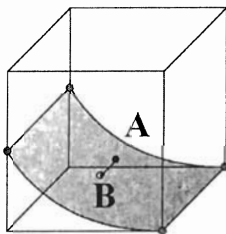

Fig. 1. Schematic diagram of determining the point 'B' for calculating the deposition rate of each surface patches.

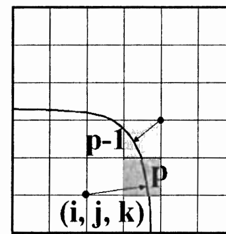

Fig. 2. Schematic diagram of determining the deposition rate of level set function.

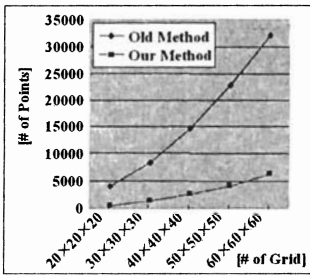

Fig. 3. Plot illustrating the comparison of our new method with old method.

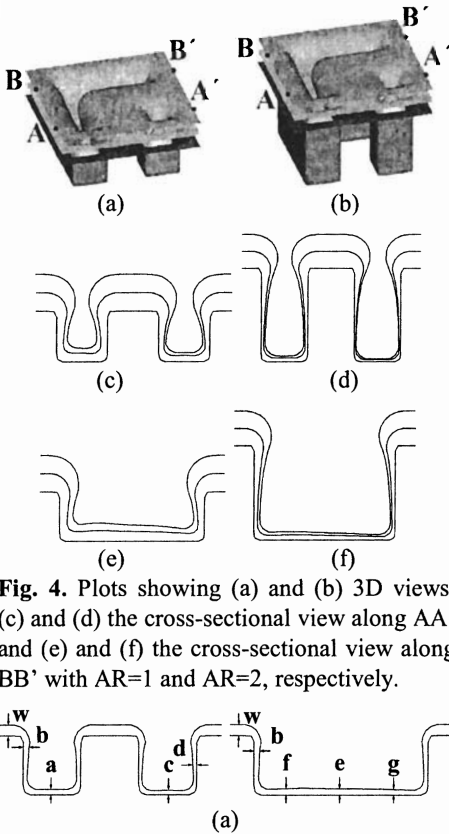

Fig. 4. Plots showing (a) and (b) 3D views, (c) and (d) the cross-sectional view along AA', and (e) and (f) the cross-sectional view along BB' with AR=1 and AR=2, respectively.

(a)

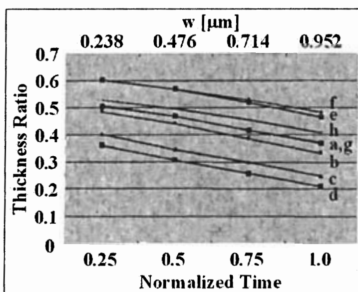

(b)

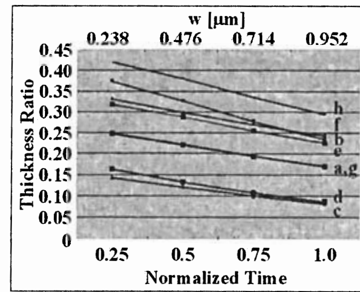

(c)

Fig. 5. Schematic diagrams illustrating (a) the locations of our interest for comparison of the thickness ratios, (b) the thickness with the aspect ratio of 1, and (c) the thickness ratio with the aspect ratio of 2.

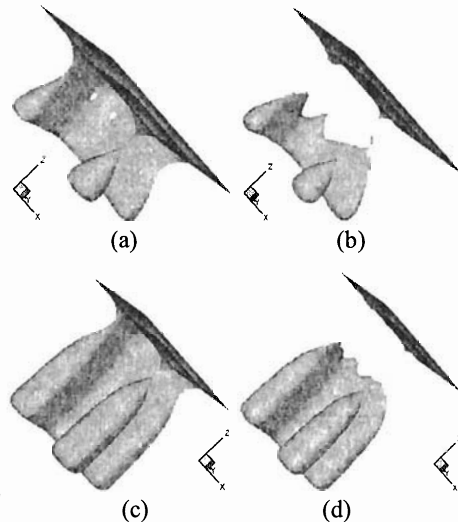

Fig. 6. Plots showing void creation (a) AR=1 and after 0.6T, (b) AR=1 and after T, (c) AR=3 and after 0.3T, and (d) AR=3 and after 0.6T.

References

[1] E. Bär and J. Lorenz, Proc. SISPAD '99, 75 (1999).

[2] J. A. Sethian, Level Set Methods (Cambridge University Press, USA, 1996).

[3] Youngchan Ban, *et al.*, J. Korean Phys. Soc., 35, S829 (1999).